Ultrasonic nanoemulsification of *Aloe vera*: formulation, optimization, and characterization.

Andrea Catalina Hernández Muñoz, Sandra Milena Echeverry, Diana Marcela Aragón Novoa*

Departamento de Farmacia, Facultad de Ciencias, Universidad Nacional de Colombia, Bogotá D.C., Colombia

Received: March 15, 2022*; Accepted:* May 20, 2022

Article Type

ABSTRACT

Aloe vera is a widely used plant in the pharmaceutical and cosmetic industry due to its anti-inflammatory, healing, moisturizing, antioxidant, anti-aging, and depigmentation properties, several of which have been attributed to the Aloesin, a compound found in the gel. This work aimed to develop an *Aloe vera* nanoemulsion for the potential use in the pharmaceutical or cosmetics industries. A Box-Behnken experimental design was used to optimize the Aloesin extraction conditions, evaluating the effect of the solvent, time, and the speed of agitation using a high shear homogenizer. After identifying the nanoemulsification zone in a pseudo-ternary diagram, a new Box-Behnken design was proposed to optimize the sonication-assisted nanoemulsification conditions (amount of surfactant, sonication time, and sonication amplitude). The optimized extract had 24% more Aloesin than the freeze-dried *Aloe vera* crystals. The optimized nanoemulsions had a dispersed phase droplet size below 200 nm, a polydispersity index of 0.200, and a zeta potential of -20 mV.

KEY WORDS: Aloesin, Box-Behnken design, pseudo-ternary diagram, nanoemulsion

INTRODUCTION

Aloe vera has elongated, jagged shaped green leaves joined at the stem in a rosette pattern and belongs to the Liliaceae family (1). The leaf cortex constitutes between 20% and 30% of the total plant weight, while the inner gel makes up 70% to 80% (2). *Aloe vera* has been reported to have several biological activities, such as wound healing, laxative effects, anti-inflammatory, anticancer, antidiabetic, and antimicrobial actions. In addition, aloe gel has moisturizing, antioxidant, anti-aging, and depigmentation properties, making it a desirable ingredient in the cosmetic industry (1-5).

*Corresponding address: Diana Marcela Aragón, Departamento de Farmacia, Facultad de Ciencias, Universidad Nacional de Colombia, Bogotá D.C., Colombia. Email: dmaragonn@unal.edu.co

The constituents of the principal *Aloe vera* are water, polysaccharides, phenolic compounds, such as anthraquinones, anthrones, chromones, flavonoids, and flavonols, and other components, such as enzymes, minerals, and essential amino acids, saponins, sterols, and vitamins (1). Aloesin, shown in Figure 1, a chromone that has shown pharmaceutical and cosmetic activity, is one of the major compounds of *Aloe vera*. In the pharmaceutical field, Aloesin has shown promising anticancer and skin wound healing effects (6, 7). In the cosmetics field, it has antioxidant activity and inhibits tyrosinase, an enzyme involved in the synthesis of melanin (4-6). Unlike other melanin inhibitors, such as hydroquinone and kojic acid, Aloesin has a good safety profile. Jones *et. al.* evaluated the integrity of cell lines that had been treated with Aloesin. The results showed

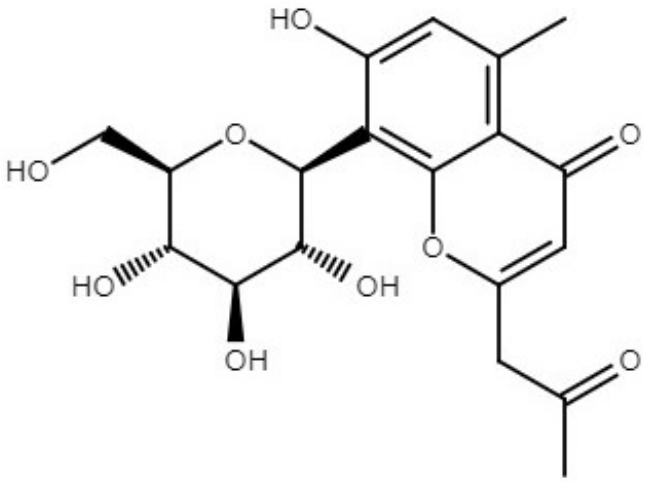

Figure 1 Chemical structure of Aloesin

no morphological abnormalities or cytotoxicity, and the melanocytes appeared normal, with multiple dendrites (7). Another study on subchronic toxicity established a No Observed Adverse Effect Level (NOAEL) of 1000 mg/kg/day for Aloesin (8).

Nanoemulsions have a droplet size of less than 500 nm and are formed in two phases, one dispersed into the other, with the help of a stabilizing agent, often a surfactant (9). Nanoemulsions can form water-in-oil or oil-in-water. Additionally, multiple or multiphase nanoemulsions can be formed. Nanoemulsions are kinetically stable but thermodynamically unstable, usually requiring a substantial amount of energy for their formation (10, 11). There are several methods for producing nanoemulsions, such as low-energy, high-energy, and combined methods. High-energy methods result in small droplet sizes, they include nanoemulsions manufactured using ultrasound based on the cavitation mechanism that produces bubbles which collapse, forming droplets (11). This method has been investigated for the production of nanoemulsions for different applications (11-14). Nanoemulsions have good skin permeation characteristics due to their small droplet size. For this reason, they are often used in topical applications (14, 15, 19, 20). This study aimed to develop a nanoemulsion that contains an *Aloe vera* extract optimized for Aloesin, for the use in the pharmaceutical or cosmetics industries.

MATERIALS AND METHODS

Plant material

Aloe vera leaves (10 kg) were purchased from a local market in the city of Bogota. The cortex was removed, the inner gel was homogenized in a laboratory blender, and the remaining water was sublimed by freeze-drying. Freeze-dried *Aloe vera* was saved as the raw extraction material.

Chemicals

HPLC-grade acetonitrile (Merck) and ultrapure water (Milli-Q® System Millipore) were used for the high-performance liquid chromatography (HPLC) analysis. Aloesin (Santa Cruz Biotechnology, Inc) was used as an analytical standard. Ethanol 99.5% (PanReac AppliChem) was used for the extraction. The sesame oil, Span® 85, and TWEEN® 20 used to produce the nanoemulsions were purchased from Sigma-Aldrich.

Aloesin extraction

Aloesin quantification by HPLC-DAD

An Agilent Infinity 1260 HPLC with DAD and Phenomenex Luna® 5 μm C18 (2) (150 x 4.6 mm) column was used. The column temperature was 45°C, a mixture of water and acetonitrile was used as the mobile phase in a gradient elution (min 0, 90:10; min 9, 82:18; min 14, 77:23; min 25, 70:30; min 30, 50:50; min 35, 50:50; min 37, 90:10; min 40, 90:10), 10 μL of sample at 1 mL/min flow were injected. Detection was performed at 300 nm; chromatograms were analyzed by OpenLAB-CDS software.

Aloesin extraction optimization

A Box-Behnken response surface design was created using the statistical software program MiniTab® 18. The design had three central points and factors, with three levels, each one for fifteen experimental runs in total. The ethanol percentage, UltraTurrax® speed range, and extraction time were evaluated. For each run, the samples were prepared as follows: 500 mg

of lyophilized aloe gel was dissolved in 40 mL in each solvent (ethanol, water, or mixture). An UltraTurrax® T18 basic IKA was used for the extraction process.

Each sample was centrifuged (Centrifuge Z 206 A, HERMLE®); the supernatant was collected, the residue was discarded, and the solvent was evaporated using a CentriVap® (LABCONCO). Five mg of the dry extract was dissolved in 1 mL of methanol. The samples were shaken and filtered through a 0.45 μm membrane, and 2 injections per sample were analyzed by HPLC-DAD.

Formulation of the nanoemulsion

Construction of the pseudo ternary diagram

Twenty-four nanoemulsions were prepared, with variations of between 4% and 20% for the sesame oil, between 4 and 24% for the surfactant (Span® 85 (65.1%), and TWEEN® 20 (34.9%) mixture), and different oil:surfactant ratios (Table 1). The surfactant quantities were established according to the required HLB value for sesame oil (HLBr = 7) and the HLB of each surfactant (Span® 85 = 1.8, TWEEN® 20 = 16.7). The emulsions were prepared using a Q500 sonicator

Table 1 Composition of the emulsions used to construct the pseudo ternary diagram.

EMULSION #	% OIL PHASE	% SURFACTANT		% AQUEOUS PHASE	OIL:SURFACTANT RATIO
		SPAN® 85	TWEEN® 20		
1	4.00	5.21	2.79	88.00	1:2
2	4.00	7.81	4.19	84.00	1:3
3	4.00	10.42	5.58	80.00	1:4
4	4.00	13.02	6.98	76.00	1:5
5	4.00	15.62	8.38	72.00	1:6
6	8.00	2.60	1.40	88.00	2:1
7	8.00	5.21	2.79	84.00	1:1
8	8.00	7.81	4.19	80.00	2:3
9	8.00	10.42	5.58	76.00	1:2
10	8.00	13.02	6.98	72.00	2:5
11	8.00	15.62	8.38	68.00	1:3
12	12.00	2.60	1.40	84.00	3:1
13	12.00	5.21	2.79	80.00	3:2
14	12.00	7.81	4.19	76.00	1:1
15	12.00	10.42	5.58	72.00	3:4
16	12.00	13.02	6.98	68.00	3:5
17	12.00	15.62	8.38	64.00	1:2
18	16.00	2.60	1.40	80.00	4:1
19	16.00	5.21	2.79	76.00	2:1
20	16.00	7.81	4.19	72.00	4:3
21	16.00	10.42	5.58	68.00	1:1
22	20.00	2.60	1.40	76.00	5:1
23	20.00	5.21	2.79	72.00	5:2
24	20.00	7.81	4.19	68.00	5:3

Table 2 Box-Behnken experimental design factors and levels for nanoemulsion optimization.

RUN	OIL: SURFACTANT RATIO	% OIL	FACTORS		
			SURFACTANT (%)	TIME (min)	AMPLITUDE (W)
1	1:0.50	8.00	4.00	5	70
2 *	1:0.75	8.00	6.00	5	80
3 *	1:0.75	8.00	6.00	5	80
4	1:1	8.00	8.00	5	90
5	1:1	8.00	8.00	6	80
6	1:1	8.00	8.00	5	70
7	1:0.50	8.00	4.00	6	80
8 *	1:0.75	8.00	6.00	5	80
9	1:0.75	8.00	6.00	4	90
10	1:0.75	8.00	6.00	6	90
11	1:0.75	8.00	6.00	4	70
12	1:1	8.00	8.00	4	80
13	1:0.75	8.00	6.00	6	70
14	1:0.50	8.00	4.00	5	90
15	1:0.50	8.00	4.00	4	80

* Central points

(QSONICA SONICATORS) sonicated for 4 minutes at 80% amplitude.

Optimization of the nanoemulsion

A Box-Behnken response surface design was created using the statistical software program MiniTab® 18. The design had three central points and three factors with three levels each, for a total of fifteen experimental runs (the same design as used in the Aloesin extraction). The oil:surfactant ratio (expressed as percentage of surfactant), emulsification time, and sonicator amplitude were evaluated (Table 2). Each emulsion was prepared using a Q500 sonicator. The optimized extract was added to each emulsion.

Characterization of the nanoemulsions

The droplet size, polydispersity index (PDI), and zeta potential of each emulsion were measured using a Zetasizer® Nano ZS (Malvern). For this, 3 μL of emulsion were removed, and deionized water was added to *q.s* to 1 mL. Measurements were performed on day 1 and day 7.

RESULTS AND DISCUSSION

Analytical method

For the analytical method, the linearity and selectivity parameters were evaluated. The selectivity was proven through all-longitude wave scanning with DAD. It was observed that at 300 nm and in the Aloesin retention time, no other compounds absorbed, the peak purity was also analyzed. A calibration curve was used for the evaluation of linearity. The results were analyzed by the ANOVA model, demonstrating that the 1 – 20 μg/mL range was linear.

Aloesin extraction

There are different extraction techniques for natural products, for example percolation, soxhlet, ultrasound-assisted, and mechanical extraction (17). High-speed homogenizers were used for the mechanical extraction. This technique is suitable for compound extraction because high yields are obtained with less solvent and a reduced time (18). The volume of plant material is reduced in this process while the target compounds are extracted with an appropriate solvent (19). Ultra-Turrax is a high shearing homogenizer that is used in different industries (cosmetics, pharmaceuticals, food, and others) for solid-liquid or liquid-liquid dispersions, and is useful in extractions as well.

For the reasons mentioned above, extraction by an Ultra-Turrax® homogenizer was chosen. The ethanol and water extraction solvent were selected based on previous research (20-25) that evaluated the best solvents for aloe compounds. Some studies have reported that water was the best solvent for extraction, while others have suggested that organic solvents such as methanol or ethanol would be optimal. An experimental design was proposed to evaluate which extraction conditions are the most suitable for obtaining the highest Aloesin concentration; the results are shown in Table 3.

Figure 2 shows the increase of Aloesin at high ethanol

Table 3 Aloesin content for each extract of the optimization design

EXTRACT #	ETHANOL (%)	SPEED RANGE (RPM)	TIME (min)	ALOESIN CONCENTRATION (µg/mg EXTRACT)
1	0	20000	8	3.760
2	100	11000	8	7.676
3	50	11000	12	3.394
4	100	15500	12	6.119
5	100	20000	8	6.854
6	50	15500	8	2.575
7	0	11000	8	3.224
8	50	20000	4	4.602
9	50	11000	4	3.296
10	0	15500	4	3.000
11	100	15500	4	10.183
12	0	15500	12	3.492
13	50	15500	8	3.433
14	50	20000	12	3.486
15	50	15500	8	3.701

percentages, regardless of the speed range. The same behavior can be observed in Figure 3, where the best Aloesin concentration was obtained with 100% ethanol and an extraction time of 4 minutes. Although the literature indicates that the ethanol:water mixture is the best solvent to extract phenolic compounds, these results show that more Aloesin can be extracted with absolute ethanol (23, 26). This can be attributed to the fact that Aloesin is more soluble in ethanol than in water. As shown in Figure 4, a high-speed range yields better Aloesin concentrations using shorter extraction times. An increase in revolutions per minute enhances the contact surface between the plant material and the solvent, due to the reduction in particle size (27). It is crucial to consider that when using a high-shear homogenizer, the temperature increases considerably over time, and this increase in temperature may not favor Aloesin stability, resulting in lower concentrations (Figure 3) (28). Other researchers suggested that lower extraction times are associated with better yields (19, 23, 27, 29).

The ANOVA (Table 4) shows that the model is significant (p-value < 0.05) while the lack-of-fit is not, so there is no evidence that the model does not fit the data. In addition, the determination coefficient (R^2) was 0.9615; the closer R^2 is to 1, the better the model fits the data. Equation 1 describes the behavior of the Aloesin amount (µg/mg extract) as response variable.

$$\begin{aligned}\text{Aloesin} = {} & 0.64 + 0.0294F1 + 0.000136\ F2 + 0.014\ F3 + \\ & 0.000829\ F1*F1 + 0.000000\ F2*F2 + \\ & 0.0243\ F3*F3 - 0.000002\ F1*F2 - \\ & 0.00570\ F1*F3 - 0.000017\ F2*F3\end{aligned} \quad \text{Eq. 1}$$

where, F1: Ethanol (min), F2: Speed range (RPM), and F3: Time (min).

According to the ANOVA results (Table 4), it is concluded that the ethanol percentage, its square, and the Ethanol (%)*Time (min) interaction are the significant factors in the Aloesin extraction. These results corroborate the analysis of Figures 2 and 3.

Response optimization establishes the optimal conditions for obtaining the highest Aloesin concentration. To check the model-predicted response (9.753 ± 2.814 µg/mg extract), five extracts were prepared under the optimal model conditions. The actual concentration was within the acceptance range (8.165 ± 2.284 µg/mg extract), indicating that the prediction model describes the extracted concentration accurately. Hence, the optimal extraction conditions selected were 100% ethanol, 20000 RPM for 4 minutes.

Formulation of the nanoemulsion

Construction of the pseudo ternary diagram

A pseudo-ternary diagram is a tool used to establish the nanoemulsification zone when the aqueous phase, oil phase, surfactants, and oil:surfactant ratio vary (30). Therefore, twenty-four nanoemulsions were prepared, based on previous studies (30–32). Sonication, a high-energy method, was chosen as the preparation method. The droplet size (nm) and PDI obtained for each emulsion are shown in Table 5. The percentage for each phase, surfactant, and oil:surfactant ratio is

Table 4 Analysis of variance of the model for Aloesin extraction optimization

SOURCE	DF	SS	MS	*F*-VALUE	*P*-VALUE *
Model	9	62.5631	6.9515	13.89	0.005
Lineal	3	40.4390	13.4797	26.94	0.002
Ethanol (%)	1	37.6519	37.6519	75.25	0.000
Speed range (rpm)	1	0.1549	0.1549	0.31	0.602
Time (min)	1	2.6321	2.6321	5.26	0.070
Square	3	16.1050	5.3683	10.73	0.013
Ethanol (%)*Ethanol (%)	1	15.8666	15.8666	31.71	0.002
Speed range (rpm)*Speed range (RPM)	1	0.0176	0.0176	0.04	0.859
Time (min)*Time (min)	1	0.5588	0.5588	1.12	0.339
Two-way interaction	3	6.0192	2.0064	4.01	0.085
Ethanol (%)*Speed range (rpm)	1	0.4611	0.4611	0.92	0.381
Ethanol (%)*Time (min)	1	5.1893	5.1893	10.37	0.023
Speed range (rpm)*Time (min)	1	0.3688	0.3688	0.74	0.430
Error	5	2.5019	0.5004		
Lack-of-fit	2	1.8104	0.6035	1.75	0.384
Pure error	1	0.6916	0.3458		
Total	14	65.0651			

DF = Degrees of freedom; SS = Sum of square; MS = Mean square * Significance level = 0.05

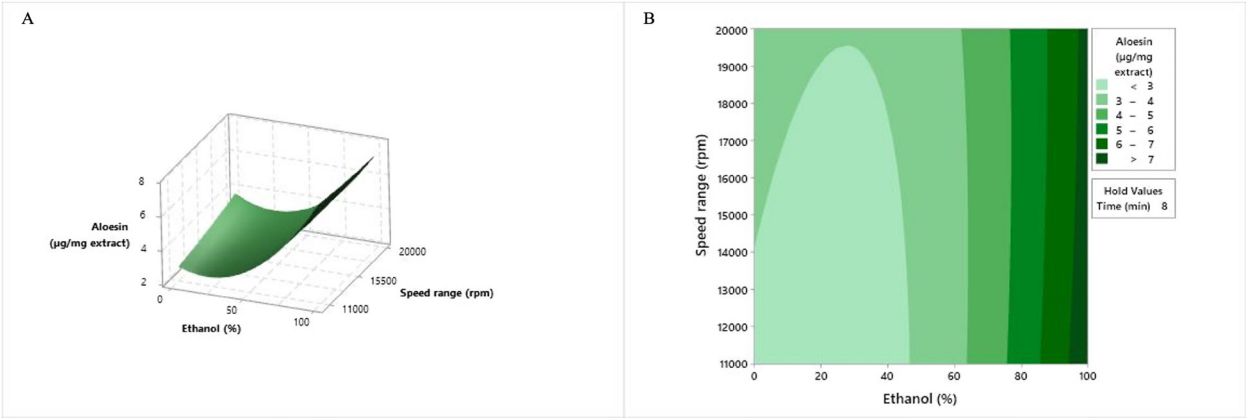

Figure 2 Response surface (A) and contour plot (B) of Aloesin (µg/mg in extract) as a function of ethanol percentage and speed range, maintaining the time factor at a constant medium level (8 minutes).

Table 5 Size (nm) and PDI values for each emulsion in the pseudo-ternary diagram.

EMULSION #	% O	% S	% A	O:S	DAY 1		DAY 7	
					Droplet size (nm)	PDI	Droplet size (nm)	PDI
1	4	8	88	1:2	215.03	0.311	216.20	0.330
2	4	12	84	1:3	243.90	0.422	204.47	0.304
3	4	16	80	1:4	206.23	0.317	269.43	0.443
4	4	20	76	1:5	234.37	0.381	249.63	0.271
5	4	24	72	1:6	210.77	0.271	225.80	0.244
6	8	4	88	2:1	271.47	0.383	205.43	0.246
7	8	8	84	1:1	249.40	0.402	209.80	0.317
8	8	12	80	2:3	228.67	0.349	231.10	0.373
9	8	16	76	1:2	236.10	0.382	200.50	0.223
10	8	20	72	2:5	207.33	0.221	201.70	0.223
11	8	24	68	1:3	218.17	0.279	231.83	0.297
12	12	4	84	3:1	255.33	0.345	303.57	0.416
13	12	8	80	3:2	217.57	0.230	312.10	0.404
14	12	12	76	1:1	205.43	0.221	210.67	0.196
15	12	16	72	3:4	216.00	0.272	203.40	0.188
16	12	20	68	3:5	201.40	0.223	198.60	0.197
17	12	24	64	1:2	184.15	0.160	202.37	0.233
18	16	4	80	4:1	325.30	0.410	337.57	0.413
19	16	8	76	2:1	333.03	0.471	340.63	0.436
20	16	12	72	4:3	231.80	0.299	256.77	0.351
21	16	16	68	1:1	286.33	0.389	214.43	0.228
22	20	4	76	5:1	356.73	0.458	316.40	0.382
23	20	8	72	5:2	237.30	0.278	255.37	0.298
24	20	12	68	5:3	276.50	0.363	218.97	0.385

O = Oil phase, S = Surfactant, A = Aqueous phase, O:S = Oil:Surfactant ratio

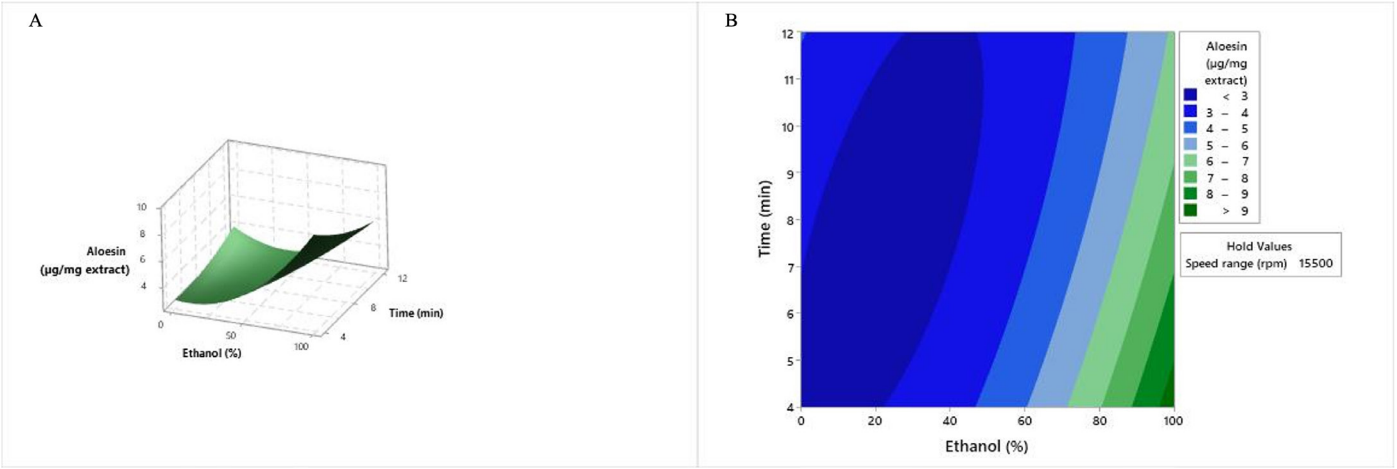

Figure 3 Response surface (A) and contour plot (B) of Aloesin (µg/mg in extract) as a function of time and ethanol percentage, maintaining the speed range factor at a constant medium level (15500 rpm).

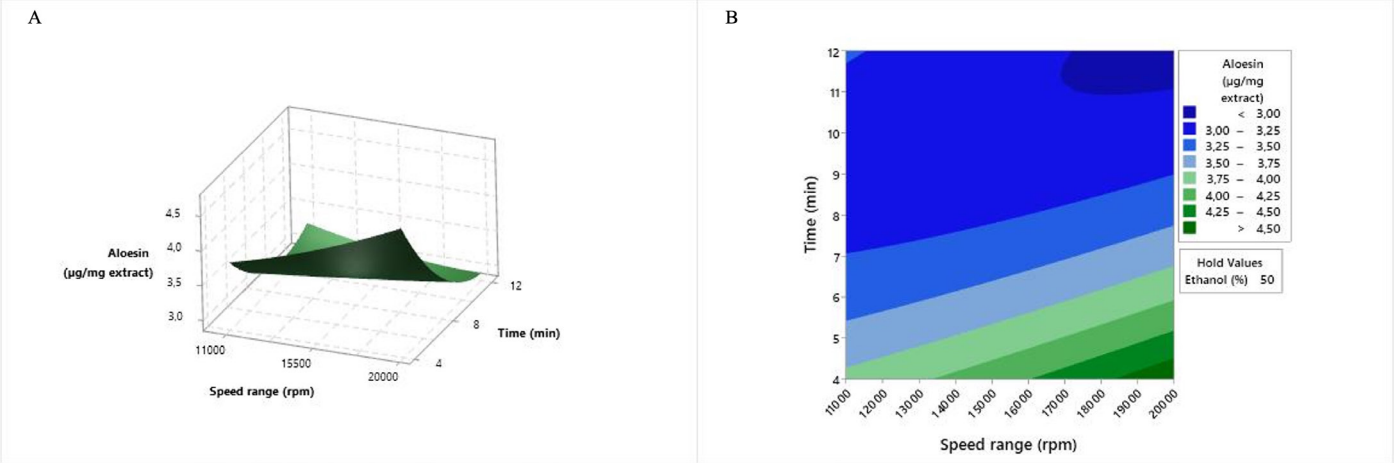

Figure 4 Response surface (A) and contour plot (B) of Aloesin (µg/mg in extract) as a function of time and speed range, maintaining the ethanol factor at a constant medium level (50%).

also shown.

The ingredients for the nanoemulsion preparation were chosen according to the literature reports for that type of product. Vegetable oils are widely used in nanoemulsions (13), and sesame oil benefits the skin, acting as an occlusive moisturizer (36). TWEEN® and Span® are non-ionic surfactants, which are preferred for skin products due to their lower toxicity compared to ionic surfactants (9, 15, 30, 34).

Although all the emulsions had a droplet size of less than 500 nm and a PDI lower than 0.500, only those with a droplet size of 250 nm or less and PDI less than or equal to 0.300 after day 7 were included in the pseudo-ternary diagram, to optimize the nanoemulsions, seeking to obtain even smaller droplet sizes. Figure 5 shows the nanoemulsification zone with an oil phase percentage between 4 – 16%, surfactant 12 – 24%, and aqueous phase 64 – 76%. Atypical data are observed with 8% oil phase, 4% surfactant, and 88% water. These results corroborate other, similar reports (31, 32).

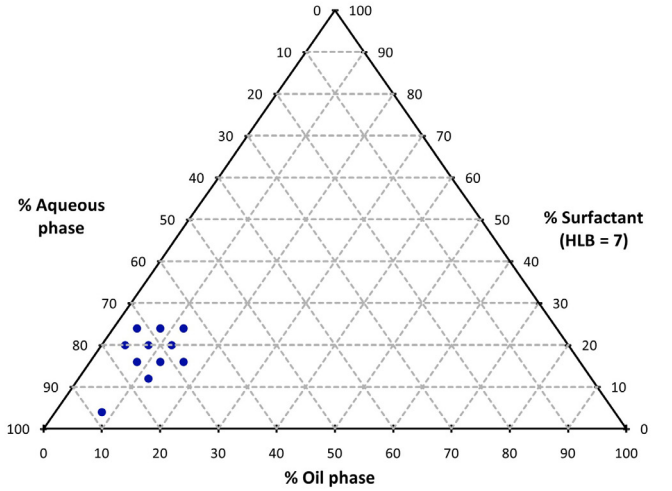

Figure 5 Pseudo ternary diagram showing the nanoemulsification zone for the evaluated formulations.

Optimization of the nanoemulsion

Having established the nanoemulsification zone, it was then possible to perform the Box-Behnken design, to optimize the conditions for preparation of the nanoemulsion, seeking to obtain the smallest possible droplet size and PDI. Based on the pseudo-ternary diagram (Figure 5), it was decided to fix the oil phase at 8% because the nanoemulsion with the lowest surfactant percentage was obtained with that amount. A maximum surfactant level of 8% was set for the experimental design, due to the concentration found in skin products; for cosmetic products in particular, the lowest possible surfactant percentage is desirable because of its irritant potential (35–37). Additionally, it has been reported that a 5% to 10% surfactant is sufficient to stabilize a 20% oil in an O/W nanoemulsion (9). Table 6 shows the results obtained for each nanoemulsion obtained through the experimental design; zeta potential was measured

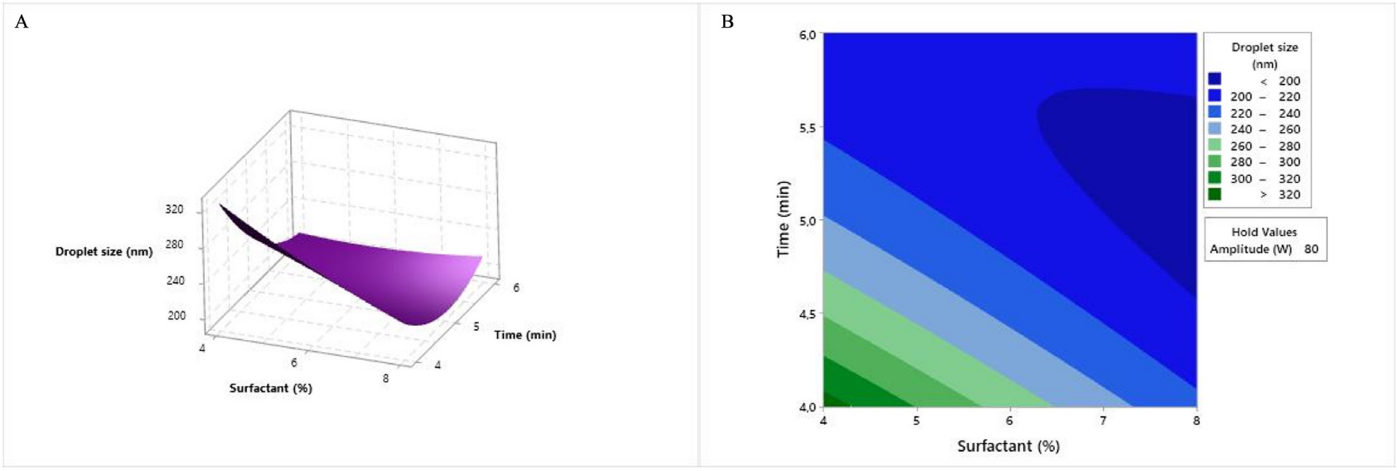

Figure 6 Response surface (A) and contour plot (B) of droplet size (nm) as a funtion of surfactant percentage and time, mainting the amplitude factor at a constant medium level (80 W).

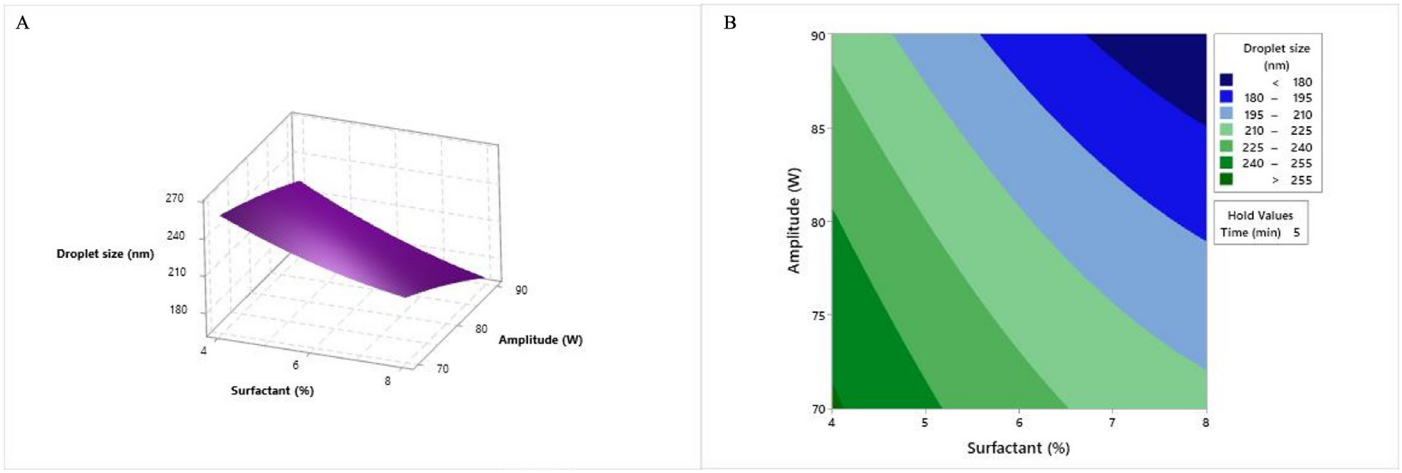

Figure 7 Response surface (A) and contour plot (B) of droplet size (nm) as a funtion of surfactant percentage and amplitude, mainting the time factor at a constant medium level (5 min).

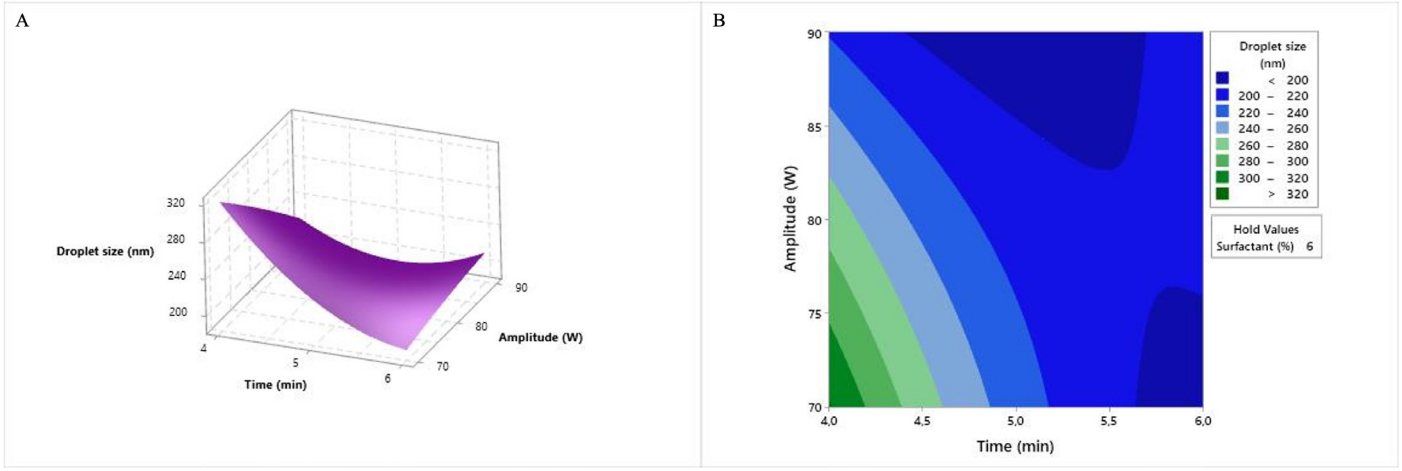

Figure 8 Response surface (A) and contour plot (B) of droplet size (nm) as a function of time and amplitude, maintaining the surfactant factor at a constant medium level (6%).

but not optimized, because the critical potential for the system is unknown. According to the results of the measurements on days 1 and 7, it was established that there are no significant differences between both measurements, and that the emulsions were sufficiently stable to coalescence during this storage period.

In general, it was observed that lower droplet sizes were obtained at higher amplitude and surfactant percentages (Figures 6-8). These results are consistent with previous studies (30, 31) because smaller droplets are formed when the percentage of surfactant is higher. On the other hand, when the sonication amplitude increases, this results in a smaller droplet size, because a higher amount of energy is supplied. In the ultrasound method, high-frequency ultrasound waves are applied with a sonotrode, and the supplied energy creates mechanical vibration and acoustic cavitation (42). The ultrasound waves cross the emulsion system, creating cavitation bubbles that implode, resulting in smaller droplets (11, 38). The time behavior on droplet size shows a range that leads to smaller droplet sizes (Figures 6 and 8). When the time value is maintained, no curvature is observed in the response (Figure 7), indicating that time is an essential factor in the response. Other studies have demonstrated the amplitude and a time at which the droplet size is no longer reduced. Therefore, it is necessary to determine the amplitude and time points that produce a significant change in droplet size (9, 11).

Mainly, small PDI values were obtained (Table 6), indicating a uniform droplet size and higher system stability because if there are big and small droplets together (PDI > 0.500), the Ostwald ripening phenomenon is favored. Ostwald ripening consists of a coarsening of droplet texture over time, resulting in coalescence and phase separation (10). However,

Table 6 Size (nm), PDI, and zeta potential values for each experimental design emulsion

EMULSION #	% O	% S	% A	O:S	DAY 1			DAY 7		
					Droplet size (nm)	PDI	Zeta potential (mV)	Droplet size (nm)	PDI	Zeta potential (mV)
1	8	4	84	1:0.50	235.90	0.251	-18.5	244.53	0.377	-27.8
2	8	6	80	1:0.75	200.23	0.219	-18.5	205.67	0.243	-18.2
3	8	6	80	1:0.75	221.37	0.248	-22.4	234.57	0.299	-19.0
4	8	8	76	1:1	187.97	0.199	-16.3	192.90	0.229	-17.7
5	8	8	76	1:1	195.77	0.201	-16.1	197.23	0.258	-15.5
6	8	8	76	1:1	213.00	0.233	-15.0	218.57	0.316	-15.3
7	8	4	84	1:0.50	209.47	0.207	-18.8	231.07	0.308	-18.1
8	8	6	80	1:0.75	213.33	0.266	-18.8	268.63	0.417	-16.4
9	8	6	80	1:0.75	199.87	0.224	-22.3	214.77	0.270	-17.8
10	8	6	80	1:0.75	209.17	0.256	-17.2	191.20	0.225	-18.6
11	8	6	80	1:0.75	325.43	0.442	-17.4	247.73	0.385	-18.6
12	8	8	76	1:1	222.50	0.290	-15.7	201.37	0.252	-20.0
13	8	6	80	1:0.75	210.70	0.245	-21.5	264.97	0.372	-17.1
14	8	4	84	1:0.50	222.87	0.266	-20.3	291.27	0.383	-21.9
15	8	4	84	1:0.50	346.47	0.459	-25.9	389.53	0.462	-18.5

O = Oil phase, S = Surfactant, A = Aqueous phase, O:S = Oil:Surfactant ratio

it must be noted that Ostwald ripening occurs by the dissolution of the disperse phase from the smaller droplets into the continuous phase followed by diffusion of the disperse phase into the larger droplets. This requires the disperse phase to have a relatively large solubility in water. Furthermore, a linear plot of (droplet diameter)^3 versus time is indicative of Ostwald ripening. Hence, the lesser PDI not favoring Ostwald ripening in the nanoemulsion must be considered speculative. Figure 9 shows that when the amplitude value is maintained, the time determines the PDI value, given that lower values are obtained over longer times, regardless of the surfactant percentage. The same situation occurs when the surfactant value is maintained, and at all amplitudes, lower PDI values are obtained (Figure 11). On the other hand, Figure 10 shows the same behavior as Figure 7, and no curvature is observed. All the PDI results are expected because the ultrasound emulsification method allows uniform droplet sizes to be obtained, due to the high energy it provides to the system (38).

Zeta potential is a measure of droplet interaction and is used as a parameter to evaluate the stability of the nanoemulsion (12). For nanoemulsions prepared with non-ionic surfactants, zeta potential values around -20 mV are reported in the literature that are potentially sufficient to provide stability to the system (12, 15). The zeta potential values obtained (Table 6) were very close to -20 mV. To obtain such values, the surfactant

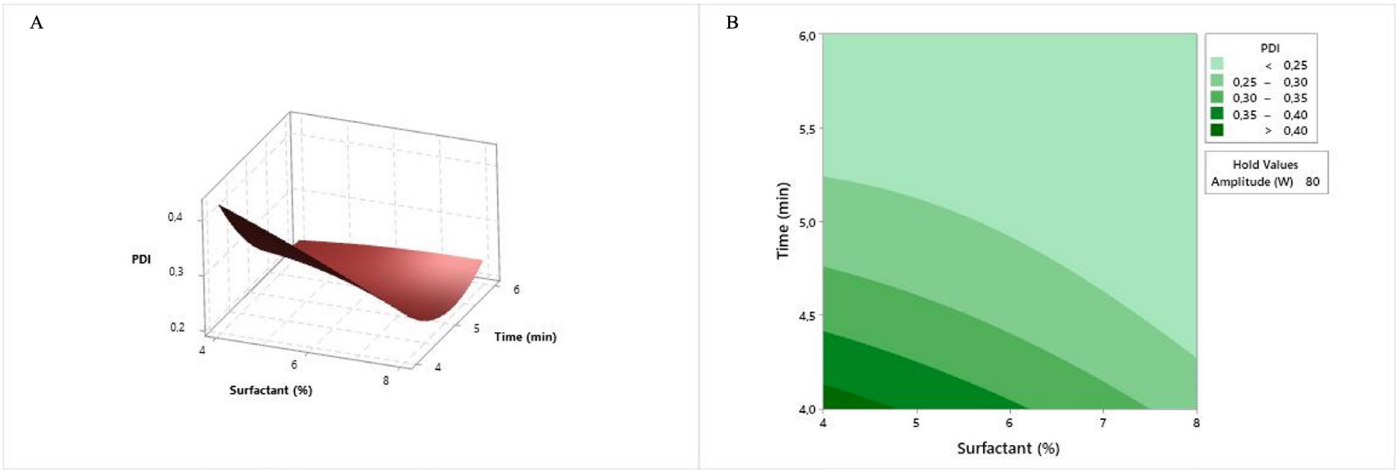

Figure 9 Response surface (A) and contour plot (B) of PDI as a function of surfactant percentage and time, maintaining the amplitude at a constant medium level (80 W).

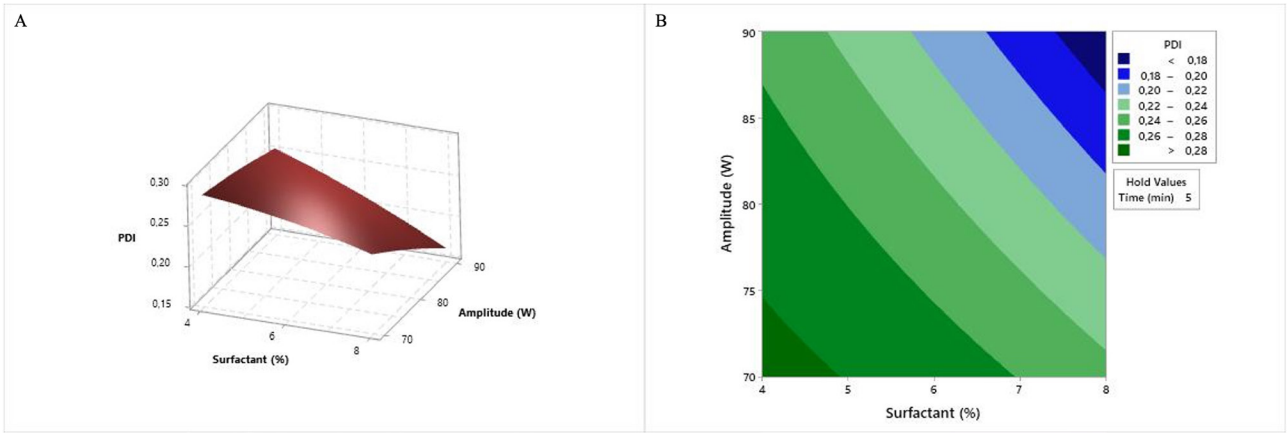

Figure 10 Response surface (A) and contour plot (B) of PDI as a function of surfactant percentage and amplitude, maintaining the time factor at a constant medium level (5 min).

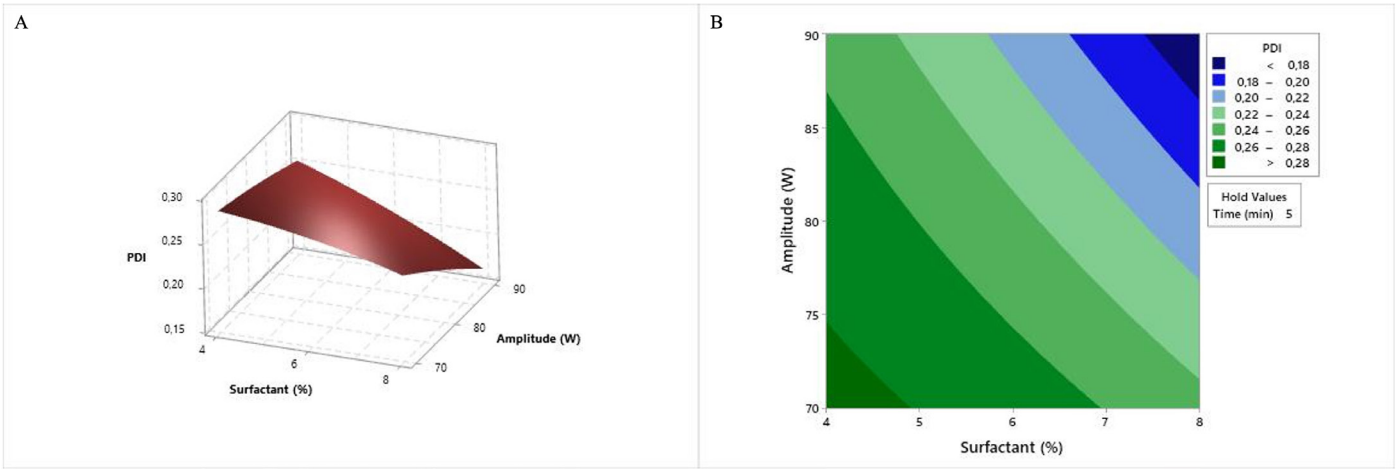

Figure 11 Response surface (A) and contour plot (B) of PDI as a function of time and amplitude, maintaining the surfactant factor at a constant medium level (6%).

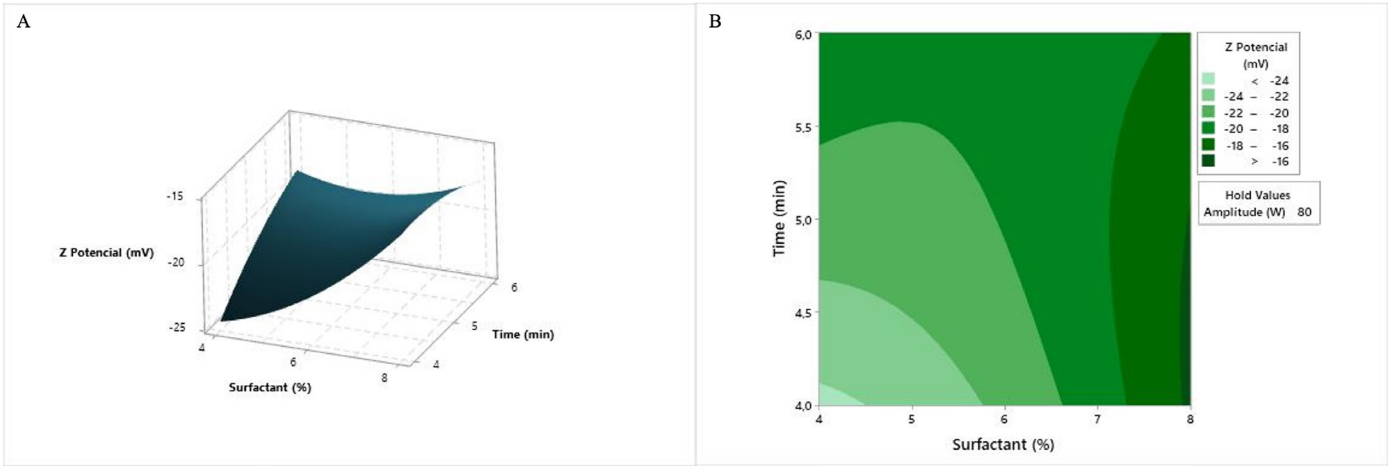

Figure 12 Response surface (A) and contour plot (B) of zeta potential as a function of surfactant percentage and time, maintaining the amplitude at a constant medium level (80 W).

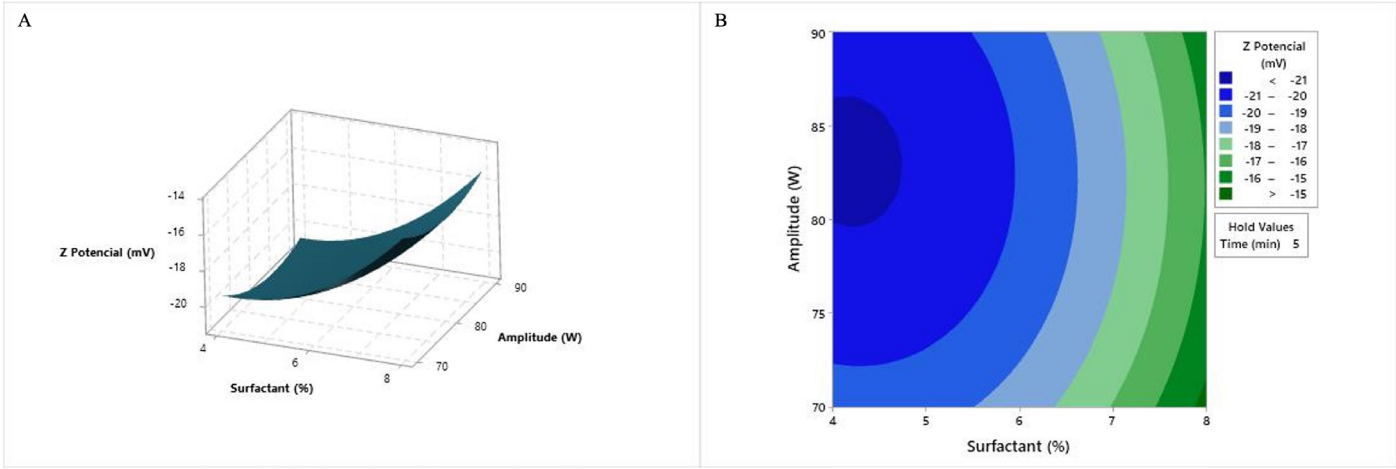

Figure 13 Response surface (A) and contour plot (B) of zeta potential as a function of surfactant percentage and amplitude, maintaining the time factor at a constant medium level (5 min).

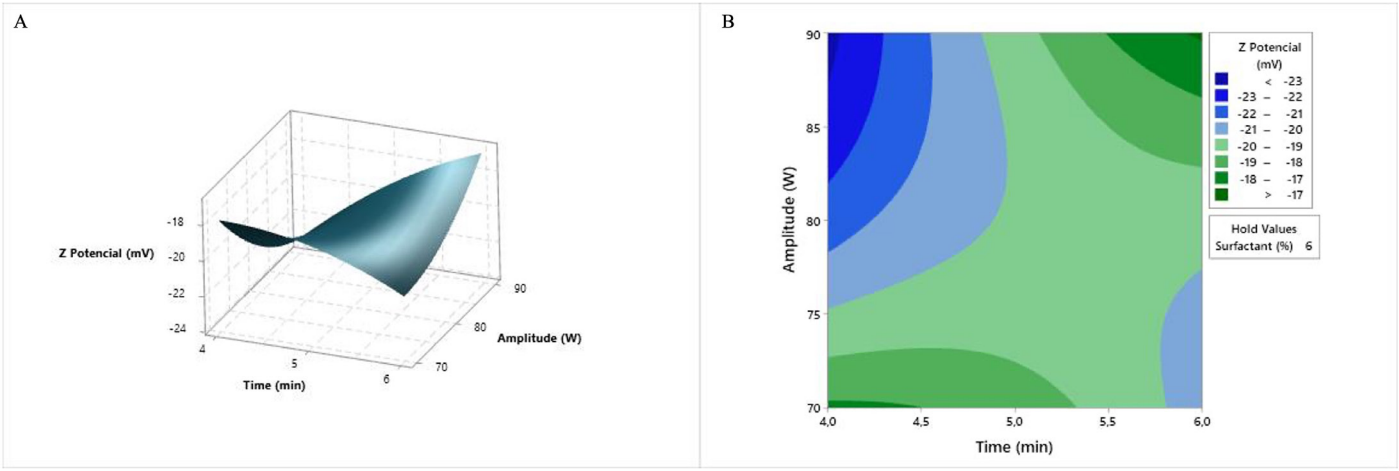

Figure 14 Response surface (A) and contour plot (B) of zeta potential as a function of time and amplitude, maintaining the surfactant factor at a constant medium level (6%).

percentage appears to be the most important factor, according to the model analysis, represented in Figures 12 and 13, showing these values are obtained at a specific surfactant percentage range regardless of the time and amplitude, respectively. Figure 13 also shows this behavior, as the curvature that forms when the surfactant percentage value is maintained.

The regression equations that describe droplet size, PDI, and potential zeta responses are presented below (Equations 2-4). According to ANOVA, the model for droplet size response was significant ($p<0.05$). On the other hand, for the lack-of-fit, the p-value was higher than 0.05, and the coefficient of determination (R^2) was 0.9168, indicating that the model correctly explains the variability of this variable response.

$$\text{Droplet size (nm)} = 2786 - 85.0\,A - 631\,B - 13.5\,C + 1.32\,A^*A + 26.6\,B^*B - 0.020\,C^*C + 13.78\,A^*B - 0.150\,A^*C + 3.10\,B^*C \quad \text{Eq .2}$$

$$\text{PDI} = 4.54 - 0.054\,A - 1.141\,B - 0.0240\,C - 0.00124\,A^*A + 0.0496\,B^*B - 0.000024\,C^*C + 0.0204\,A^*B - 0.00062\,A^*C + 0.00573\,B^*C \quad \text{Eq. 3}$$

$$\text{Zeta Potential (mV)} = 93.8 + 1.10\,A - 5.0\,B - 2.72\,C + 0.355\,A^*A - 0.665\,B^*B + 0.00935\,C^*C - 0.929\,A^*B + 0,0071\,A^*C + 0,2275\,B^*C \quad \text{Eq. 4}$$

where, A = Surfactant (%), B = Time (min), and C = Amplitude (W)

For the PDI and zeta potential response, the R^2 was lower than for droplet size (R^2 = 0.8808 and 0.8589, respectively). In addition, the model for both responses had a p-value > 0.05, indicating that the model is not significant. However, there is no evidence that the model does not fit the data, because the lack-of-fit value is higher than 0.05 (see Table 7).

The ANOVA analysis indicated that for droplet size, all the individual factors (surfactant percentage, amplitude, and time) and Time (min)*Amplitude (W) interaction are significant in the nanoemulsification process. For the PDI and zeta potential responses, only the time and surfactant percentage are significant, respectively. The optimization result indicates that the values of each factor needed to obtain the lowest droplet size are: 8% surfactant, 4.5 min, and 90 W. Five nanoemulsions were prepared to check the droplet size response predicted by the software (161.0 ± 77.2 nm). The droplet size obtained experimentally (188.3 ± 4.6 nm) was within the predicted response, indicating that the model prediction is reasonable. Additionally, the PDI and zeta potential values obtained were 0.205 ± 0.013 and -20.4 mV ± 1.0, respectively, and therefore within the desired values.

Table 7 Analysis of variance for the nanoemulsification optimization model

Source	DF	DROPLET SIZE (nm)				PDI				ZETA POTENTIAL (mV)			
		SS	MS	*F*-value	*p*-value*	SS	MS	*F*-value	*p*-value*	SS	MS	*F*-value	*p*-value*
Model	9	26889.3	2987.70	6.12	0.030	0.076721	0.008525	4.10	0.067	108.006	12.0006	3.38	0.097
Lineal	3	17242.2	5747.41	11.77	0.011	0.046816	0.015605	7.51	0.027	60.860	20.2867	5.72	0.045
A	1	4775.9	4775.90	9.78	0.026	0.008450	0.008450	4.07	0.100	52.020	52.0200	14.66	0.012
B	1	9056.3	9056.34	18.55	0.008	0.031962	0.031962	15.39	0.011	7.220	7.2200	2.03	0.213
C	1	3410.0	3410.00	6.99	0.046	0.006403	0.006403	3.08	0.139	1.620	1.620	0.46	0.529
Square	3	2725.3	908.44	1.86	0.254	0.009498	0.003166	1.52	0.317	12.549	4.1831	1.18	0.406
A * A	1	102.7	102.69	0.21	0.666	0.000090	0.000090	0.04	0.843	7.425	7.4248	2.09	0.208
B * B	1	2618.8	2618.81	5.36	0.068	0.009098	0.009068	4.38	0.091	1.634	1.6342	0.46	0.528
C* C	1	14.5	14.54	0.03	0.870	0.000021	0.000021	0.01	0.925	3.226	3.2260	0.91	0.384
Two-way interaction	3	6921.8	2307.25	4.73	0.064	0.020407	0.006802	3.27	0.117	34.596	11.5321	3.25	0.119
A * B	1	3039.7	3039.68	6.23	0.055	0.006642	0.006642	3.20	0.134	13.814	13.8136	3.89	0.106
A * C	1	36.0	36.00	0.07	0.797	0.000617	0.000617	0.30	0.609	0.080	0.0803	0.02	0.886
B * C	1	3846.1	3846.07	7.88	0.038	0.013148	0.013148	6.33	0.053	20.702	20.7025	5.83	0.060
Error	5	2440.7	488.13			0.010386	0.002077			17.747	3.5494		
Lack-of-fit	3	2213.1	737.69	6.48	0.137	0.009245	0.003082	5.40	0.160	8.419	2.8065	0.60	0.673
Pure error	2	227.6	113.79			0.001142	0.000571			9.327	4.6637		
Total	14	29330.0				0.087108				125.753			

A = Surfactant, B = Time, C = Amplitude, DF = Degrees of freedom; SS = Sum of square; MS = Mean square * Significance level = 0.05

CONCLUSIONS

Optimum extraction conditions for extracting Aloesin from *Aloe vera* gel were established. The Box-Behnken design enabled the optimal extraction conditions to be established in order to obtain the greatest Aloesin concentration at 100% ethanol with a 20000 RPM speed range and time of 4 minutes. The pseudo-ternary diagram construction helped determine the nanoemulsification zone, in order to identify the conditions for nanoemulsion preparation and obtain the smallest droplet size. These conditions were optimized using a surface response methodology. The results showed that with an 8% surfactant, and using a sonotrode with amplitude = 90 W for 4.5 minutes, it was possible to obtain nanoemulsions with droplet sizes of less than 200 nm and PDI less than 0.300. The formulation developed is promising for its potential use in the pharmaceutical or cosmetics industries due to the advantages of the small droplet size in the nanoemulsion, its stability for at least 7 days, and its reported *Aloe vera* properties. Finally, the formulation must be evaluated in terms of long-term stability, biological activity and skin safety in future investigations.

ACKNOWLEDGEMENTS

The authors wishes to acknowledge the Pharmacy Department of Universidad Nacional de Colombia for the supply of equipment and the use of its facilities during this study.

REFERENCES

1 Minjares-Fuentes R, Femenia A. Chapter 3.4 - *Aloe Vera*. In Nonvitamin and Nonmineral Nutritional Supplements; Nabavi, S. M., Silva, A. S., Eds., Academic Press, pp 145–152, 2019.

2 Domínguez-Fernández R, Arzate-Vázquex I, Chanona-Pérez J, Welti-Chanes J, Alvarado-González J, Calderón-Domínguez G, Garibay-Febles V, Gutiérrez-López G. El Gel de Aloe Vera: Estructura, Composición Química, Procesamiento, Actividad Biológica e Importancia En La Industria Farmacéutica y Alimentaria. Revista Mexicana de Ingeniería Química, 11(1): 23–43, 2012.

3 Wahedi H, Jeong M, Chae J, Do S, Yoon H, Kim S. Aloesin from Aloe Vera Accelerates Skin Wound Healing by Modulating MAPK/Rho and Smad Signaling Pathways in Vitro and in Vivo. Phytomedicine: International Journal of Phytotherapy and Phytopharmacology, 28: 19–26, 2017.

4 Mukherjee PK, Biswas R, Sharma A, Banerjee S, Biswas S, Katiyar CK. Validation of Medicinal Herbs for Anti-Tyrosinase Potential. Journal of Herbal Medicine, 14: 1–16, 2018.

5 Zhu W, Gao J. The Use of Botanical Extracts as Topical Skin-Lightening Agents for the Improvement of Skin Pigmentation Disorders. Journal of Investigative Dermatology Symposium Proceedings, 13(1): 20–24, 2008.

6 Clark AK, Sivamani RK. Phytochemicals in the Treatment of Hyperpigmentation. Botanics: Targets and Therapy, 6: 89–96, 2016.

7 Jones K, Hughes J, Hong M, Jia Q, Orndorff S. Modulation of Melanogenesis by Aloesin: A Competitive Inhibitor of Tyrosinase. Pigment Cell Research, 15(5): 335–340, 2002.

8 Lynch B, Simon R, Roberts A. Subchronic Toxicity Evaluation of Aloesin. Regulatory Toxicology and Pharmacology, 61(2): 161–171, 2011.

9 Shah MR, Imran M, Ullah S. Chapter 4 - Nanoemulsions. In Lipid-Based Nanocarriers for Drug Delivery and Diagnosis; Shah, M. R., Imran, M., Ullah, S., Eds.; William Andrew Publishing, pp 111–137, 2017.

10 Sonneville-Aubrun O, Yukuyama MN, Pizzino A. Chapter 14 - Application of Nanoemulsions in Cosmetics. In Nanoemulsions; Jafari, S. M., McClements, D. J., Eds.; Academic Press, pp 435–475, 2018.

11 Yukuyama MN, Ghisleni DDM, Pinto TJA, Bou-Chacra NA. Nanoemulsion: Process Selection and Application in Cosmetics – a Review. International Journal of Cosmetic Science, 38(1): 13–24, 2016.

12 Ugur Kaplan AB, Cetin M, Orgul D, Taghizadehghalehjoughi A, Hacımuftuoglu A, Hekimoglu S. Formulation and in Vitro Evaluation of Topical Nanoemulsion and Nanoemulsion-Based Gels Containing Daidzein. Journal of Drug Delivery Science and Technology, 52: 189–203, 2019.

13 Saberi AH, Fang Y, McClements DJ. Fabrication of Vitamin E-Enriched Nanoemulsions: Factors Affecting Particle Size Using Spontaneous Emulsification. Journal of Colloid and Interface Science, 391(1): 95–102, 2013.

14 Campani V, Biondi M, Mayol L, Cilurzo F, Pitaro M, de Rosa G. Development of Nanoemulsions for Topical Delivery of Vitamin K1. International Journal of Pharmaceutics, 511(1): 170–177, 2016.

15 Rai VK, Mishra N, Yadav KS, Yadav NP. Nanoemulsion as Pharmaceutical Carrier for Dermal and Transdermal Drug Delivery: Formulation Development, Stability Issues, Basic Considerations and Applications. Journal of Controlled Release, 270: 203–225, 2018.

16 Baspinar Y, Borchert HH. Penetration and Release Studies of Positively and Negatively Charged Nanoemulsions—Is There a Benefit of the Positive Charge? International Journal of

Pharmaceutics, 430(1–2): 247–252, 2012.

17 Zhang Q-W, Lin L-G, Ye W-C. Techniques for Extraction and Isolation of Natural Products: A Comprehensive Review. Chinese Medicine, 13(1): 1–26, 2018.

18 Rocchetti G, Blasi F, Montesano D, Ghisoni S, Marcotullio M, Sabatini S, Cossignani L, Lucini L. Impact of Conventional/Non-Conventional Extraction Methods on the Untargeted Phenolic Profile of Moringa Oleifera Leaves. Food Res Int, 115: 319–327, 2019.

19 Xu WJ, Zhai JW, Cui Q, Liu JZ, Luo M, Fu YJ, Zu YG. Ultra-Turrax Based Ultrasound-Assisted Extraction of Five Organic Acids from Honeysuckle (Lonicera Japonica Thunb.) and Optimization of Extraction Process. Separation and Purification Technology, 166: 73–82, 2016.

20 Okamura N, Asai M, Hine N, Yagi A. High-Performance Liquid Chromatographic Determination of Phenolic Compounds in Aloe Species. Journal of Chromatography A, 746(2): 225–231, 1996.

21 Dell'Agli M, Giavarini F, Ferraboschi P, Galli G, Bosisio E. Determination of Aloesin and Aloeresin A for the Detection of Aloe in Beverages. Journal of Agricultural and Food Chemistry, 55(9): 3363–3367, 2007.

22 Baek M, Jeong J, Kim D. Determination of Aloesin in Rat Plasma Using a Column-Switching High-Performance Liquid Chromatographic Assay. J Chromatogr B Biomed Sci Appl, 754(1): 121–126, 2001.

23 Kim S, Asnin L, Assefa AD, Ko EY, Sharma K, Park SW. Extraction of Antioxidants from Aloe Vera Leaf Gel: A Response Surface Methodology Study. Food Analytical Methods, 7(9): 1804–1815, 2014.

24 Nazeam J, Gad H, El-Hefnawy H, Singab A. Chromatographic Separation and Detection Methods of Aloe Arborescens Miller Constituents: A Systematic Review. J Chromatogr B Analyt Technol Biomed Life Sci, 1058: 57–67, 2017.

25 Zhan M, Trinh T, Jeong M, Wang D, Abeysinghe P, Jia Q, Ma W. A Reversed-Phase High-Performance Liquid Chromatographic Method for the Determination of Aloesin, Aloeresin A and Anthraquinone in Aloe Ferox. Phytochem Anal, 19(2): 122–126, 2008.

26 Muñoz W, Chavez W, Pabón LC, Rendón MR, Patricia-Chaparro M, Otálvaro-Álvarez ÁM. Extracción de Compuestos Fenólicos Con Actividad Antioxidante a Partir de Champa (*Campomanesia Lineatifolia*). Revista CENIC Ciencias Químicas, 46: 38–46, 2015.

27 Sari F, Velioglu YS. Effects of Particle Size, Extraction Time and Temperature, and Derivatization Time on Determination of Theanine in Tea. Journal of Food Composition and Analysis, 24(8): 1130–1135, 2011.

28 Scholz P, Keck CM. Nanoemulsions Produced by Rotor–Stator High Speed Stirring. International Journal of Pharmaceutics, 482(1–2): 110–117, 2015.

29 Sepúlveda PM, Echeverrry S, Costa G, Aragón M. Passiflora Ligularis Leaf Ultrasound-Assisted Extraction in the Optimization of Flavonoid Content and Enhancement of Hypoglycemic Activity. Journal of Applied Pharmaceutical Science, 10(8): 86–94, 2020.

30 Elmataeeshy ME, Sokar MS, Bahey-El-Din M, Shaker DS. Enhanced Transdermal Permeability of Terbinafine through Novel Nanoemulgel Formulation; Development, in Vitro and in Vivo Characterization. Future Journal of Pharmaceutical Sciences, 4(1): 18–28, 2018.

31 Hernández-Rivera JA, Martínez-Ramírez JA, Rojas-Cardozo M, Aragón Novoa DM. Evaluation of Passiflora Tripartita Var. Mollissima Seed Oil as Potential Nanoemulsion Excipient. Journal of Excipients and Food Chemicals, 9(1): 16–27, 2018.

32 Guzmán C, Rojas MA, Aragón M. Optimization of Ultrasound-Assisted Emulsification of Emollient Nanoemulsions of Seed Oil of Passiflora Edulis Var. Edulis. Cosmetics, 8(1): 2021.

33 Warra A. Sesame (*Sesamum Indicum* L.) Seed Oil Methods of Extraction and Its Prospects in Cosmetic Industry: A Review. Bayero Journal of Pure and Applied Sciences, 4(2): 164–168, 2012.

34 Lawrence MJ, Rees GD. Microemulsion-Based Media as Novel Drug Delivery Systems. Advanced Drug Delivery Reviews, 64(SUPPL.): 175–193, 2012.

35 Lémery E, Briançon S, Chevalier Y, Bordes C, Oddos T, Gohier A, Bolzinger MA. Skin Toxicity of Surfactants: Structure/Toxicity Relationships. Colloids and Surfaces A: Physicochemical and Engineering Aspects, 469: 166–179, 2015.

36 Seweryn A. Interactions between Surfactants and the Skin – Theory and Practice. Advances in Colloid and Interface Science, 256: 242–255, 2018.

37 Effendy I, Maibach HI. Surfactants and Experimental Irritant Contact Dermatitis. Contact Dermatitis, 33(4): 217–225, 1995.

38 Páez-Hernández G, Mondragón-Cortez P, Espinosa-Andrews H. Developing Curcumin Nanoemulsions by High-Intensity Methods: Impact of Ultrasonication and Microfluidization Parameters. LWT - Food Science and Technology, 111: 291–300, 2019.